IEEE Photonics Journal
An IEEE Photonics Society Publication

Photonic Generation of Multilevel Frequency-Hopping Microwave Signal

Volume 11, Number 1, February 2019

Xia Feng
Lianshan Yan
Hengyun Jiang
Peng Li
Jia Ye
Yin Zhou
Wei Pan
Bin Luo
Xihua Zou
Tao Zhou

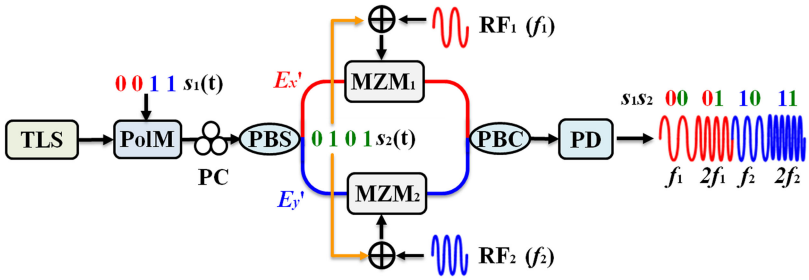

DOI: 10.1109/JPHOT.2018.2885943
1943-0655 © 2017 IEEE

Photonic Generation of Multilevel Frequency-Hopping Microwave Signal

Xia Feng,[1] **Lianshan Yan**,[1] **Hengyun Jiang**,[1] **Peng Li**,[1] **Jia Ye**,[1] **Yin Zhou**,[1] **Wei Pan**,[1] **Bin Luo**,[1] **Xihua Zou**,[1] **and Tao Zhou**[2]

[1]Center for Information Photonics and Communications, School of Information Science and Technology, Southwest Jiaotong University, Chengdu 611756, China
[2]Key Laboratory of Electronic Information Control, Southwest China Research Institute of Electronic Equipment, Chengdu 610036, China

DOI:10.1109/JPHOT.2018.2885943

Manuscript received October 25, 2018; revised December 2, 2018; accepted December 6, 2018. Date of publication December 10, 2018; date of current version January 1, 2019. This work was supported in part by the National Natural Science Foundation of China under Grants 61335005, 61860206006, and 61771438; and in part by the Ministry of Education United Foundation of Equipment Pre-Research under Grant 6141A020334. Corresponding author: L. Yan (e-mail: lsyan@home.swjtu.edu.cn).

Abstract: A photonic scheme to generate a 4-level frequency hopping (FH) microwave signal is proposed and experimentally demonstrated. The frequency of the generated signal can be fast and flexibly switched by shifting the combinations of two binary signals (i.e., 00, 01, 11, 10). Moreover, the carrier frequencies of the signal can be tuned in a large range. In the experiments, 2/4/6/12, 4/6/8/12, and 6/9/12/18 GHz FH signals are generated with the FH speed up to gigahertz.

Index Terms: Frequency hopping, microwave signal generation, radio frequency photonics, analog optical signal processing.

1. Introduction

Frequency hopping (FH) microwave signal has been widely used in the wireless communication, radar and electronic countermeasures systems, due to its inherent characteristics such as zero inter-symbol interference and anti-jamming [1]–[3]. Due to the electronic bottleneck of the traditional electrical methods, the bandwidth and FH speed of the signals are limited to few GHz and MHz, respectively. Nowadays, the photonic generation of microwave signals has been considered as a promising alternation owing to its broad bandwidth, large tunability, low loss, and immunity to electromagnetic interference [4]–[6].

Up to now, quite a few photonic approaches to generate FH microwave signals have been proposed. One way to generate a 2-level FH microwave signal is realized by controlling the bias points of optical modulators [7]–[10]. Another way is implemented by utilizing a polarization maintaining fiber Bragg grating (PM-FBG) and a polarization modulator (PolM) based on the polarization-dependent frequency response of the PM-FBG [11], [12]. However, the frequency agility is limited due to the use of optical filter. In practical applications, multi-level FH signals are more desirable. In Refs. [13], [14], a method to generate multi-level FH microwave signals is proposed based on the pulse shaping and frequency to time mapping. However, the system is complicated and costly due to the use of optical pulse shaper and the mode-locked laser (MLL). Another method to generate multi-level FH microwave signals is realized based on the optical delay self-heterodyne which consists

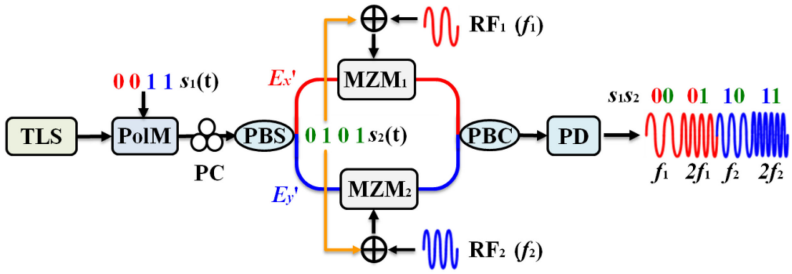

Fig. 1. Conceptual diagram of the proposed 4-level FH microwave signal generation. TLS, tunable laser source; PolM, polarization modulator; PC, polarization controller; PBS, polarization beam splitter; MZM, Mach-Zehnder modulator; PBC, polarization beam combiner; PD, Photo-detector.

of an unbalance Mach-Zehnder interferometer together with a wavelength-swept distributed Bragg reflector (DBR) laser or distributed feedback (DFB) laser [15], [16]. The FH speed is determined by the wavelength sweeping speed of the laser. Two lasers of a wavelength-swept DFB laser and a fixed wavelength laser are used to generate multi-level FH microwave signals [17]. However, two incoherent optical sources may degrade the quality of the generated signal. An optically injected semiconductor laser based on the period-one oscillation is proposed to generate the multi-level FH signals that are determined by the optical injected strength [18]–[20]. In Ref. [21], an optical tunable filter implemented by a thermally tuning silicon micro-ring resonator is used to generate a multi-level FH signal with the FH speed of 2-kHz.

In this letter, a photonic scheme to generate a 4-level FH microwave signal with high FH speed (~GHz) and large frequency tunability is proposed. In the scheme, a PolM combined with a polarization beam splitter (PBS) is used to divide an optical carrier into two branches by controlling a binary signal $s_1(t)$. For each branch, a radio frequency signal is applied to a Mach-Zehnder modulator (MZM) biased by a binary signal $s_2(t)$. Then, a 4-level FH microwave signal can be realized. The frequency of the generated signal can be switched flexibly by controlling the two binary signals. The FH speed is determined by the bit rates of the two binary signals. In the proof-of-concept experiment, 4-level FH signals with tunable carrier frequencies and different FH speeds are generated.

2. Principle and Theoretical Analysis

The conceptual diagram of the proposed scheme is shown in Fig. 1, which consists of a tunable laser source (TLS), a PolM, a PBS, two MZMs, a polarization beam combiner (PBC) and a photo-detector (PD). A light wave from the TLS is sent to a PolM driven by a binary signal $s_1(t)$. The optical field at the output of the PolM can be expressed as

$$E_{PolM} = \begin{bmatrix} E_x \\ E_y \end{bmatrix} = \begin{bmatrix} E_o \exp(j\omega_0 t + j\beta_1 s_1(t)) \\ E_o \exp(j\omega_0 t - j\beta_1 s_1(t)) \end{bmatrix} \tag{1}$$

where E_o and ω_o are the amplitude and angular frequency of the light wave, respectively. $\beta_1 = \pi V_1/2V_{\pi p}$, V_1 is the amplitude of the binary signal $s_1(t)$, $V_{\pi p}$ is the half-wave voltage of the PolM.

Then the output signal is sent to a PBS with its principal axis oriented at an angle of 45° to one principal axis of the PolM by using a polarization controller (PC). The output signals of the PBS can be expressed as

$$\begin{bmatrix} E_x' \\ E_y' \end{bmatrix} = \frac{\sqrt{2}}{2} \begin{bmatrix} E_x + E_y \\ E_x - E_y \end{bmatrix} = \begin{bmatrix} \sqrt{2}E_o \exp(j\omega_0 t)\cos(\beta_1 s_1(t)) \\ \sqrt{2}jE_o \exp(j\omega_0 t)\sin(\beta_1 s_1(t)) \end{bmatrix} \tag{2}$$

By adjusting the amplitude of the binary signal $s_1(t)$ properly (typically $V_1 = V_{\pi p}$, $\beta_1 = \pi/2$), the output signals can be divided into two branches with complementary amplitudes, as the control

signal $s_1(t)$ is bit '0' or '1'. The Eq. (2) can be simplified as

$$\begin{bmatrix} E_{x'} \\ E_{y'} \end{bmatrix} = \begin{cases} \begin{bmatrix} \sqrt{2}E_o \exp(j\omega_o t) \\ 0 \end{bmatrix}, & s_1(t) = 0 \\ \begin{bmatrix} 0 \\ \sqrt{2}jE_o \exp(j\omega_o t) \end{bmatrix}, & s_1(t) = 1 \end{cases} \tag{3}$$

It can be seen from Eq. (3), the combination of the PolM and the PBS is used as a fast optical switch that may be replaced by a simple dual-output Mach-Zehnder modulator. For each branch, an MZM is employed subsequently. Radio frequency signals RF_1 and RF_2 added with a binary signal $s_2(t)$, are applied to the MZM_1 and MZM_2, respectively. The output signals of the $MZM_{1,2}$ of two branches can be expressed as

$$\begin{bmatrix} E_{M1} \\ E_{M2} \end{bmatrix} = \begin{bmatrix} E_{x'} \exp(j\delta_1/2)\cos(m_1\cos(\omega_1 t) + \beta_{21}s_2(t) + \delta_1/2) \\ E_{y'} \exp(j\delta_2/2)\cos(m_2\cos(\omega_2 t) + \beta_{22}s_2(t) + \delta_2/2) \end{bmatrix} \tag{4}$$

where $m_{1,2} = \pi V_{R1,2}/2V_{\pi M1,2}$ are the modulation index of the $MZM_{1,2}$, respectively. $V_{R1,2}$, $V_{\pi M1,2}$, are the amplitudes of the $RF_{1,2}$ signals and the half-wave voltages of the $MZM_{1,2}$, respectively. $\omega_{1,2} = 2\pi f_{1,2}$ are the angular frequencies of the $RF_{1,2}$. $\beta_{2-1,2} = \pi V_{2-1,2}/2V_{\pi M1,2-d}$, $V_{2-1,2}$ are the amplitudes of binary signal $s_2(t)$ applied to the $MZM_{1,2}$, and $V_{\pi M1,2-d}$ are the half-wave direct current (DC) voltages of the $MZM_{1,2}$. $\delta_{1,2}$ are the phase differences of the $MZM_{1,2}$ caused by the bias voltage.

Then the two output signals are combined by using a PBC and then detected by a PD. The detected signal can be expressed as

$$I(t) = R(E_{M1} + E_{M2})(E_{M1} + E_{M2})^* = \begin{cases} 2RE_o^2\cos^2[m_1\cos(\omega_1 t) + \beta_{21}s_2(t) + \delta_1/2], & s_1(t) = 0 \\ 2RE_o^2\cos^2[m_2\cos(\omega_2 t) + \beta_{22}s_2(t) + \delta_2/2], & s_1(t) = 1 \end{cases} \tag{5}$$

where R is the responsivity of the PD. An expansion of Eq. (5) with Bessel function can be written as

$$I(t) = RE_o^2 \begin{cases} 1 - 2J_1(2m_1)\cos(\omega_1 t)\sin[2\beta_{21}s_2(t) + \delta_1] \\ \quad + [J_0(2m_1) - 2J_2(2m_1)\cos(2\omega_1 t)] \times \cos[2\beta_{21}s_2(t) + \delta_1], & s_1(t) = 0 \\ 1 - 2J_1(2m_2)\cos(\omega_2 t)\sin[2\beta_{22}s_2(t) + \delta_2] \\ \quad + [J_0(2m_2) - 2J_2(2m_2)\cos(2\omega_2 t) \times \cos[2\beta_{22}s_2(t) + \delta_2], & s_1(t) = 1 \end{cases} \tag{6}$$

where J_n is the nth-order Bessel function, and the higher orders are ignored. By adjusting the bias voltages of the $MZM_{1,2}$, $\delta_1 = \delta_2 = \pi/2$ can be obtained. By properly tuning the amplitude of $s_2(t)$ (typically, $V_{2-1,2} = V_{\pi M1,2-d}/2$), $\beta_{21} = \beta_{22} = \pi/4$ can be obtained. The Eq. (6) can be simplified as

$$I(t) = RE_o^2 \begin{cases} 1 - 2J_1(2m_1)\cos(\omega_1 t), & s_1(t) = 0, s_2(t) = 0 \\ 1 - J_0(2m_1) + 2J_2(2m_1)\cos(2\omega_1 t), & s_1(t) = 0, s_2(t) = 1 \\ 1 - 2J_1(2m_2)\cos(\omega_2 t), & s_1(t) = 1, s_2(t) = 0 \\ 1 - J_0(2m_2) + 2J_2(2m_2)\cos(2\omega_2 t), & s_1(t) = 1, s_2(t) = 1 \end{cases} \tag{7}$$

The frequency f_1 (or f_2) and frequency $2f_1$ (or $2f_2$) are switched when the bit data of $s_2(t)$ changes. When $s_2(t) = 1$, i.e., the $MZM_{1,2}$ works at the minimum transmission point, carrier-suppression double-sideband signals can be generated. After detection, signals with the frequency of $2f_{1,2}$ can be obtained. When $s_2(t) = 0$, i.e., the $MZM_{1,2}$ works at the quadrature transmission point with the best linear modulation characteristics. After detection, signals with the frequency of $f_{1,2}$ can be obtained.

When the amplitude of $RF_{1,2}$ signal for bit '1' is $0.5V_{\pi M1,2-d}$ (i.e., half-wave DC voltage) more than the one for bit '0', the generated FH signal with equal amplitude can be obtained (i.e., $J_1(2m_1) =$

$J_2(2m_1) = J_1(2m_2) = J_2(2m_2) = A$). Blocking the DC, the Eq. (7) can be further simplified as

$$I(t) \propto 2RA E_o^2 \begin{cases} \cos(\omega_1 t), & s_1(t) = 0, s_2(t) = 0 \\ \cos(2\omega_1 t), & s_1(t) = 0, s_2(t) = 1 \\ \cos(\omega_2 t), & s_1(t) = 1, s_2(t) = 0 \\ \cos(2\omega_2 t), & s_1(t) = 1, s_2(t) = 1 \end{cases} \tag{8}$$

It can be seen from Eq. (8), a 4-level FH microwave signal with the carrier frequencies of f_1, $2f_1$, f_2, $2f_2$ is obtained, and the frequency can be switched flexibly by controlling the combinations of two binary signals $s_1(t)$ and $s_2(t)$. In addition, each carrier frequency can be tuned by changing the $RF_{1,2}$ signals, and the FH speed depends on the bit rate of $s_{1,2}(t)$.

3. Experimental Results

An experiment is implemented to verify the proposed scheme. The experimental setup is similar to Fig. 1. PCs are added before the modulators and the PBC respectively. An optical delay line is used in the lower-branch to adjust the delay between the two branches. An erbium-doped fiber amplifier (EDFA) with a tunable gain is employed before the PD to compensate the power loss in links. The central wavelength and output power of the light wave generated from the TLS (Yenista) are set as 1550.080-nm and 12-dBm, respectively. The binary signal $s_1(t)$ is generated by a pulse-pattern generator (PPG, Anritsu, MT181). The half-wave voltage of the 40-Gb/s PolM (Versawave) is 5-V. The added signals of the binary signal $s_2(t)$ and $RF_{1,2}$ signals are directly generated by an arbitrary waveform generator (AWG, Keysight M9502A). A 40-Gb/s intensity modulator (Sumicem) with the half-wave voltage of 3.5-V is used as the MZM_1, and another 40-Gb/s intensity modulator (Osaka) with half-wave voltage of 4.5-V is used as the MZM_2. The output signal is received by a PD (Agilent 11982A) with the 3-dB bandwidth of 15-GHz. Finally, the generated FH microwave signal is monitored by a Digital Storage Oscilloscope (Keysight DSOZ634A) with the sampling rate of 80-GSa/s.

Firstly, the bit-rate of the binary signal $s_1(t)$ is set as 0.5-Gbit/s with a fixed pattern of "00110011". By properly adjusting the strength of $s_1(t)$, maximum amplitudes complementary signals from the PBS with on-off keying format are detected as shown in Fig. 2(a) and (b). When the binary signal $s_1(t)$ is bit '0' ('1'), the optical signal appears (disappears) in upper branch, disappears (appears) in the lower branch, which matches well with Eq. (3). The optical signal divides into two branches corresponding to the bit data of $s_1(t)$. Then, the bit-rate and pattern of the binary signal $s_2(t)$ are set as 0.5-Gbit/s and "01100110", respectively. The carrier frequencies of RF_1 and RF_2 are 2-GHz and 6-GHz, respectively. The electrical signals applied to the MZM_1 and MZM_2 are shown as Fig. 2(c) and (d). By tuning the bias voltage and the output RF power applied to the MZM_1, the detected signal of the upper branch before the PBC is shown in Fig. 2(e). 2-level FH signal with frequencies of 2-GHz and 4-GHz is obtained. When the binary signal $s_2(t)$ is bit '0', the MZM_1 is biased at the quadrature transmission point, and 2-GHz signal is generated. When the binary signal $s_2(t)$ is bit '1', the MZM_1 is biased at the minimum transmission point, and 4-GHz signal is generated. In the same way, the detected signal of lower branch before the PBC is shown in Fig. 2(f), a 2-level FH signal with frequencies 6-GHz and 12-GHz is obtained. The frequencies 6-GHz and 12-GHz of generated signal are corresponding to bit '0' and '1' of the binary signal $s_2(t)$, respectively. Then the 4-level FH microwave signal with the FH speed of 0.5-GHz is obtained as shown in Fig. 2(g). The carrier frequencies 2/4/6/12-GHz of the generated FH signal are corresponding to the bit arrays 00, 01, 10, 11 of $s_1(t)s_2(t)$, respectively. The feasibility of the proposed scheme is well verified.

In the following, the tunability of carrier frequency in the proposed 4-level FH microwave signal generation scheme is investigated. The carrier frequencies of RF_1 and RF_2 are tuned to be 4-GHz and 6-GHz, respectively. The patterns and bit rates of the two binary signals are unchanged. The generated 4-level FH microwave signal with carrier frequencies of 4/6/8/12-GHz is obtained as shown in Fig. 3(a). The carrier frequencies of RF_1 and RF_2 are changed as 6-GHz and 9-GHz, respectively. The generated 4-level FH microwave signal with carrier frequencies of 6/9/12/18-GHz

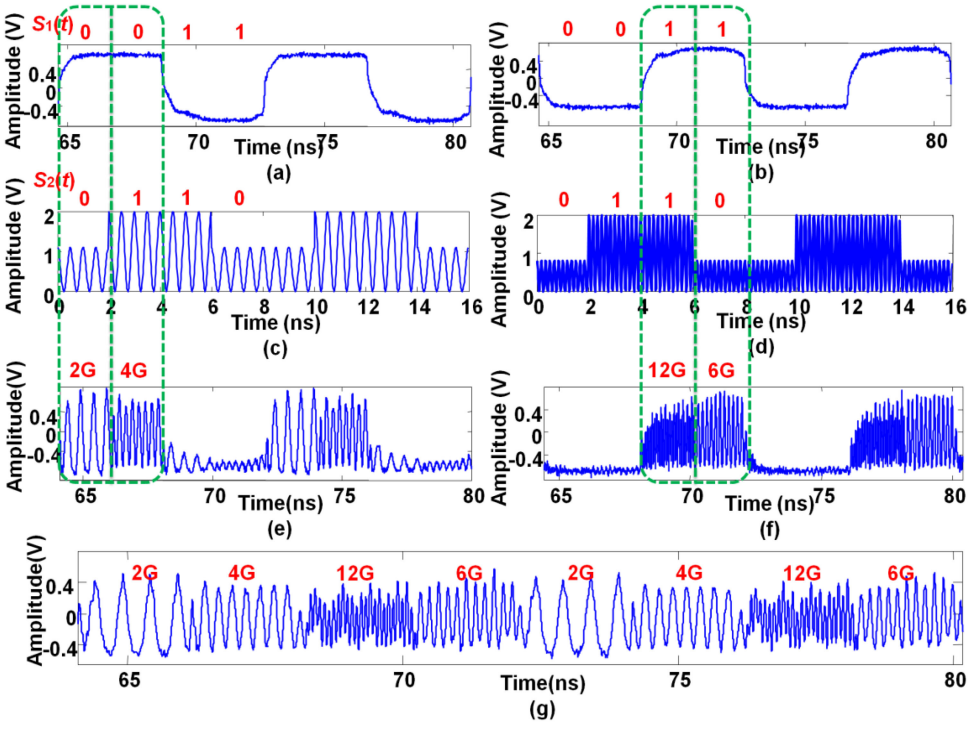

Fig. 2. Detected signals of the (a) upper and (b) lower branch after the PBS; Electrical signals applied to the (c) MZM_1 of the upper branch and (d) the MZM_2 of the lower branch; Detected signals of the (e) upper and (f) lower branch before the PBC; (g) Generated 4-level FH signal with carrier frequencies 2/4/6/12-GHz and FH speed 0.5-GHz.

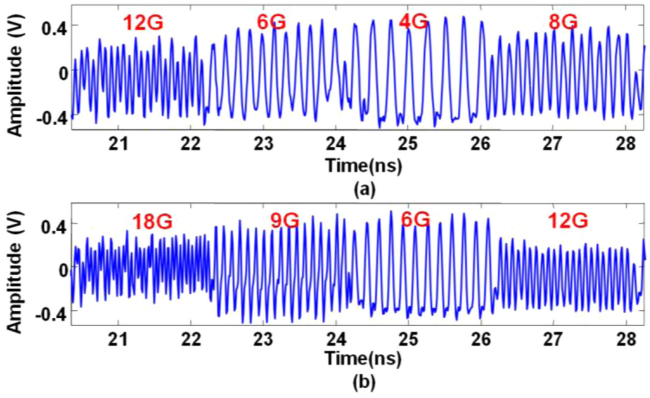

Fig. 3. (a) Generated 4-level FH signal with carrier frequencies 4/6/8/12-GHz, (b) Generated 4-level FH signal with carrier frequencies 6/9/12/18-GHz.

is obtained as shown in Fig. 3(b). It can be seen from Figs. 2(g), 3(a), and 3(b), the generated FH signals of the proposed scheme with tunable carrier frequencies are generated. In the experiments, the bandwidths of the generated signals are determined by the bandwidths of MZMs and PD.

Furthermore, the tunability of the FH speed is also experimentally demonstrated. The bit rates of the two PRBS signals are set as 1-Gbit/s. The carrier frequencies of RF_1 and RF_2 are kept as 6-GHz and 9-GHz, respectively. The generated 4-level FH signal with the carrier frequencies of 6/9/12/18-GHz is shown in Fig. 4(a). A zoom-in view of a section of the generated signal is shown in Fig. 4(b). It is obviously shown that four frequencies are switched flexibly with the FH speed of

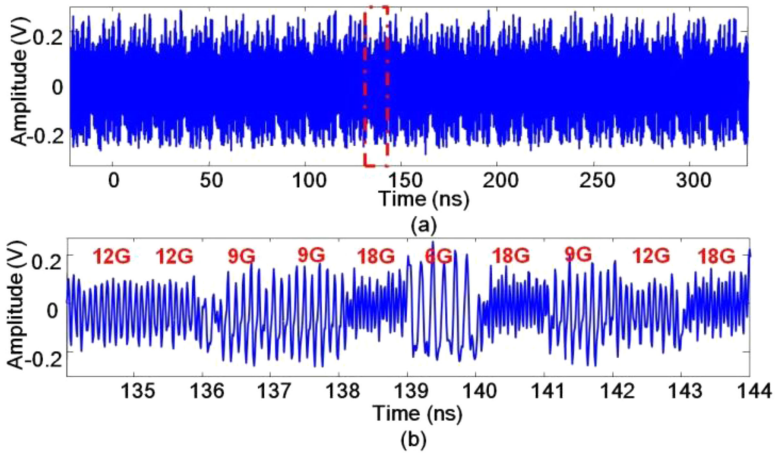

Fig. 4. (a) Generated 4-level FH signal with carrier frequencies 6/9/12/18-GHz and FH speed 1 GHz, (b) Zoom-in view of a section of the generated signal outlined in red dotted line in (a).

1-GHz. Compared with the results of Fig. 2 (or Fig. 3), the obtained FH signal still has a good performance with long bit sequences, and the FH speed of the proposed scheme is determined by the bit rates of the two binary signals.

In the experiment, the quality of generated signals may be affected by the stability of the bias of the modulators. Consequently, bias control circuits are required in practical applications.

4. Conclusion

In conclusion, a photonic scheme to generate a 4-level FH microwave signal is proposed and experimentally demonstrated. In the proposed scheme, the frequency of the generated FH signal can be fast and flexibly switched by controlling two binary baseband signals applied to the modulators. In the experiments, several sets of 4-level FH signals with different frequencies and FH speeds are generated to verify the feasibility and tunability of the proposed scheme. Such a scheme may be used in the applications of radar, wireless communication, etc.

References

[1] M. I. Skolnik, *Radar Handbook*. New York, NY, USA: McGraw-Hill, 2008.
[2] M. K. Simon, J. K. Omura, R. A. Scholtz, and B. K. Levitt, *Spread Spectrum Communications Handbook*. New York, NY, USA: McGraw-Hill, 1994.
[3] R. A. Poisel, *Introduction to Communication Electronic Warfare Systems*. Norwood, MA, USA: Artech House, 2008.
[4] J. Capmany and D. Novak, "Microwave photonics combines two worlds," *Nat. Photon.*, vol. 1, no. 6, pp. 319–330, Jun. 2007.
[5] J. Yao, "Microwave photonics," *J. Lightw. Technol.*, vol. 27, no. 3, pp. 314–335, Feb. 2009.
[6] X. Yan, X. Zou, W. Pan, L. Yan, and J. Azaña, "Fully digital programmable optical frequency comb generation and application," *Opt. Lett.*, vol. 43, no. 2, pp. 283–286, Jan. 2018.
[7] L. Huang *et al.*, "Photonic generation of microwave frequency shift keying signals," *IEEE Photon. Technol. Lett.*, vol. 28, no. 18, pp. 1928–1931, Sep. 2016.
[8] Y. Chen, "High-speed and wideband frequency-hopping microwave signal generation via switching the bias point of an optical modulator," *IEEE Photon. J.*, vol. 10, no. 1, Feb. 2018, Art. no. 5500407.
[9] H. Jiang *et al.*, "Microwave photonic comb filter with ultra-fast tunability," *Opt. Lett.*, vol. 40, no. 21, pp. 4895–4898, Nov. 2015.
[10] H. Jiang, L. Yan, W. Pan, B. Luo, and X. Zou, "Ultra-high speed RF filtering switch based on stimulated Brillouin scattering," *Opt. Lett.*, vol. 43, no. 2, pp. 279–282, Jan. 2018.
[11] J. Ye, L. Yan, H. Wang, W. Pan, B. Luo, and X. Zou, "Photonic generation of microwave frequency shift keying signal using a polarization maintaining FBG," *IEEE Photon. J.*, vol. 10, no. 3, Jun. 2018, Art. no. 5501108.
[12] J. Yao, W. Li, and W. Zhang, "Frequency-hopping microwave waveform generation based on a frequency-tunable optoelectronic oscillator," in *Proc. Int. Conf. Opt. Fiber Commun.*, San Francisco, CA, USA, 2014, Art. no. W1J–2.

[13] A. Rashidinejad and A. M. Weiner, "Achieving the upper bound time-bandwidth product for radio-frequency arbitrary waveform generation," in *Proc. Int. Top. Meet. Microw. Photon.*, Alexandria, VA, USA, 2013, pp. 186–189.
[14] A. Rashidinejad and A. M. Weiner, "Photonic radio-frequency arbitrary waveform generation with maximal time-bandwidth product capability," *J. Lightw. Technol.*, vol. 32, no. 20, pp. 3383–3393, Oct. 2014.
[15] N. Zhu, Y. Du, X. Wu, J. Zheng, H. Wang, and J. Liu, "Fast tunable and broadband microwave sweep-frequency source based on photonic technology," *Sci. China Tech. Sci.*, vol. 56, no. 3, pp. 612–616, Mar. 2013.
[16] O. L. Coutinho, J. Zhang, and J. Yao, "Photonic generation of a linearly chirped microwave waveform with a largetime-bandwidth product based on self-heterodyne technique," in *Proc. Int. Top. Meet. Microw. Photon.*, Paphos, Cyprus, 2015, pp. 1–4.
[17] J. Wun, C. Wei, J. Chen, C. S. Goh, S. Y. Set, and J. Shi, "Photonic chirped radio-frequency generator with ultra-fast sweeping rate and ultra-wide sweeping range," *Opt. Exp.*, vol. 21, no. 9, pp. 11475–11481, May 2013.
[18] P. Zhou, F. Zhang, X. Ye, Q. Guo, and S. Pan, "Flexible frequency-hopping microwave generation by dynamic control of optically injected semiconductor laser," *IEEE Photon. J.*, vol. 8, no. 6, Dec. 2016, Art. no. 5501909.
[19] N. G. Usechak, J. S. Suelzer, and J. W. Haefner, "High-speed wideband voltage-controlled oscillator via an injection-locked laser," *IEEE Photon. Technol. Lett.*, vol. 29, no. 13, pp. 1132–1135, Jul. 2017.
[20] P. Zhou, F. Zhang, Q. Guo, S. Li, and S. Pan, "Reconfigurable radar waveform generation based on an optically injected semiconductor laser," *IEEE J. Sel. Topics Quantum Electron.*, vol. 23, no. 6, Nov. 2017, Art. no. 1801109.
[21] F. Zhou *et al.*, "Frequency-hopping microwave generation with a large time-bandwidth product," *IEEE Photon. J.*, vol. 10, no. 3, Jun. 2018, Art. no. 7800809.